Development 121, 3151-3162 (1995)
Printed in Great Britain © The Company of Biologists Limited 1995

Formin isoforms are differentially expressed in the mouse embryo and are required for normal expression of *fgf-4* and *shh* in the limb bud

David C. Chan, Anthony Wynshaw-Boris* and Philip Leder

Department of Genetics, Harvard Medical School, and Howard Hughes Medical Institute, 200 Longwood Avenue, Boston, MA 02115, USA

*Present address: Laboratory of Genetic Disease Research, National Center for Human Genome Research, National Institutes of Health, Building 49/4A80, Bethesda, MD 20892, USA

SUMMARY

Mice homozygous for the recessive *limb deformity* (*ld*) mutation display both limb and renal defects. The limb defects, oligodactyly and syndactyly, have been traced to improper differentiation of the apical ectodermal ridge (AER) and shortening of the anteroposterior limb axis. The renal defects, usually aplasia, are thought to result from failure of ureteric bud outgrowth. Since the *ld* locus gives rise to multiple RNA isoforms encoding several different proteins (termed *formins*), we wished to understand their role in the formation of these organs. Therefore, we first examined the embryonic expression patterns of the four major *ld* mRNA isoforms. Isoforms I, II and III (all containing a basic amino terminus) are expressed in dorsal root ganglia, cranial ganglia and the developing kidney including the ureteric bud. Isoform IV (containing an acidic amino terminus) is expressed in the notochord, the somites, the apical ectodermal ridge (AER) of the limb bud and the developing kidney including the ureteric bud. Using a *lacZ* reporter assay in transgenic mice, we show that this differential expression of isoform IV results from distinct regulatory sequences upstream of its first exon. These expression patterns suggest that all four isoforms may be involved in ureteric bud outgrowth, while isoform IV may be involved in AER differentiation. To define further the developmental consequences of the *ld* limb defect, we analyzed the expression of a number of genes thought to play a role in limb development. Most significantly, we find that although the AERs of *ld* limb buds express several AER markers, they do not express detectable levels of *fibroblast growth factor 4* (*fgf-4*), which has been proposed to be the AER signal to the mesoderm. Thus we conclude that one or more formins are necessary to initiate and/or maintain *fgf-4* production in the distal limb. Since *ld* limbs form distal structures such as digits, we further conclude that while *fgf-4* is capable of supporting distal limb outgrowth in manipulated limbs, it is not essential for distal outgrowth in normal limb development. In addition, *ld* limbs show a severe decrease in the expression of several mesodermal markers, including *sonic hedgehog* (*shh*), a marker for the polarizing region and *Hoxd-12*, a marker for posterior mesoderm. We propose that incomplete differentiation of the AER in *ld* limb buds leads to reduction of polarizing activity and defects along the anteroposterior axis.

Key words: *limb deformity*, limb mutant, limb development, polarizing activity, apical ectodermal ridge, *shh*, *fgf-4*

INTRODUCTION

The vertebrate limb has long been a model system for studying mechanisms of pattern formation (Tabin, 1991; Tickle and Eichele, 1994). Classical embryological experiments, primarily on chick limbs, have yielded a wealth of information on how the proximodistal and anteroposterior axes of the limb are determined. Patterning along the proximodistal axis is controlled by the apical ectodermal ridge (AER), a prominent strip of thickened epithelium along the rim of the limb bud. The AER is morphologically and functionally distinct from adjacent limb ectoderm and its surgical removal from underlying limb mesoderm leads to truncation of the resulting limb (Saunders, 1948). There is a quantitative relationship between the time of AER removal and the severity of the limb truncation: progressively earlier removal of the AER results in progressively more severe truncations along the proximodistal axis (Saunders, 1948; Summerbell, 1974). These results are consistent with the 'progress zone' model, which proposes that the AER provides a constant signal to maintain the underlying mesodermal cells (in the progress zone) in an undifferentiated and proliferative state (Summerbell et al., 1973). As the limb develops, mesodermal cells constantly leave the progress zone and differentiate. Cells that leave early acquire proximal fates, while cells that leave late acquire distal fates. In this model, the amount of time spent under the influence of the AER signal determines the fate of mesodermal cells.

The zone of polarizing activity (ZPA, or polarizing region), a patch of posterior limb mesoderm, is believed to pattern mesodermal cells along the anteroposterior axis. When ZPA

tissue is transplanted into the anterior mesoderm of a host chick wing bud, the resulting limb displays a mirror-image duplication of digits (Saunders and Gasseling, 1968). Instead of the normal **2-3-4** digit pattern, the manipulated wings typically have the pattern **4*-3*-2*-2-3-4** (where * indicates duplicated digits). The ZPA has been proposed to be the source of a diffusible morphogen whose concentration gradient provides positional information for cells along the anteroposterior axis (Tickle et al., 1975).

Much progress has been made towards understanding the molecular basis of these two signaling centers of the vertebrate limb bud. *Fibroblast growth factor 4* (*fgf-4*) is expressed in the posterior AER (Niswander and Martin, 1992) and can maintain distal outgrowth in limb buds that have been stripped of the AER (Niswander et al., 1993). *Fibroblast growth factor 2* (*fgf-2*) is expressed in the AER and dorsal limb ectoderm (Savage et al., 1993) and can also replace the AER in similar assays (Fallon et al., 1994). These two growth factors are therefore molecular candidates for the signal(s) provided by the AER to support the outgrowth and undifferentiated state of the underlying mesoderm. Recent experiments suggest that FGFs may also be involved in the initiation of limb bud outgrowth from the embryonic flank (Cohn et al., 1995). *Sonic hedgehog* (*shh*), a secreted putative signaling molecule, is expressed in the polarizing region, as well as in other embryonic tissues containing ZPA activity (Echelard et al., 1993; Krauss et al., 1993; Riddle et al., 1993; Roelink et al., 1994). Cells infected or transfected with *shh*-producing vectors acquire ZPA activity, arguing strongly that *shh* is the active agent of the ZPA (Riddle et al., 1993; Chang et al., 1994).

We have approached the problem of vertebrate limb development by studying a recessive mouse mutation called *limb deformity* (*ld*) (Woychik et al., 1985). Mice homozygous for any of the five characterized *ld* mutations show reduction and fusion of digits and fusion of the distal long bones (radius/ulna, tibia/fibula). At gestational day 10.5, limb buds of *ld* embryos contain an incomplete and poorly differentiated AER and have a reduction in the anteroposterior limb axis (Zeller et al., 1989). In addition, these mice have an incompletely penetrant kidney defect, which consists of either renal aplasia (ld^{OR}, ld^{J}, ld^{TgHd}, ld^{In2} and ld^{TgBri}) or hydronephrosis (ld^{In2}) (Kleinebrecht et al., 1982; Woychik et al., 1985; Woychik et al., 1990a). The renal aplasia in ld^{J} mice has been traced to an absence or delay of ureteric bud outgrowth (Maas et al., 1994).

Cloning of the *ld* locus led to the identification of a set of novel proteins termed formins (Woychik et al., 1990b). These protein isoforms arise from alternative splicing of *ld* transcripts. Four major isoforms (I-IV) have been described for the mouse *ld* gene (Jackson-Grusby et al., 1992). These four isoforms are expressed in two distinct patterns. Ribonuclease protection analyses show that isoforms I-III, which share a common 5′ exon encoding a basic amino terminus, are coordinately expressed and are present in the embryonic kidney but not in the limb bud. In contrast, isoform IV, containing a different 5′ exon encoding an acidic amino terminus, is expressed in both the embryonic kidney and the limb bud (Jackson-Grusby et al., 1992; Maas et al., 1994). In situ hybridization experiments on embryonic sections show that expression of isoform IV in the mouse limb bud is most intense in the AER (Jackson-Grusby et al., 1992).

In this study, we examine in detail these two major embryonic expression patterns of *ld* transcripts. We find that isoforms I-III are expressed primarily in the nervous system and developing kidney, whereas isoform IV is expressed in the AER and also the developing kidney. To gain insight into the developmental defects underlying the *ld* limb phenotype, we analyzed early stage *ld* limb buds using a number of limb-specific markers. Our results show that the AER of *ld* limbs expresses several AER markers, but is poorly organized and, significantly, fails to produce *fgf-4*. Mesodermal defects in *ld* limbs include greatly reduced expression of *shh* and *Hoxd-12*.

MATERIAL AND METHODS

Preparation of embryos

For the studies of *ld* isoform expression, random-bred Swiss Webster mice were checked daily for vaginal plugs. Noon of the day of plug appearance was considered to be day 0.5. Embryos were dissected, fixed overnight in 4% paraformaldehyde, dehydrated through a methanol series and stored in methanol at −20°C till needed. During the dissections, extraembryonic membranes were saved for genotyping. For the urogenital expression studies, the urogenital system was dissected intact from embryos at days 11.5 to 16.5. These samples were then fixed and processed as for whole embryos.

Mutant *ld* embryos were obtained from timed-pregnancies resulting from homozygous *ld* females mated to either heterozygous or homozygous *ld* males. Identical results were obtained with both the ld^{In2} and ld^{TgBri} lines. Embryos were genotyped using a CA dinucleotide-repeat assay, which detects polymorphisms between the wild-type and mutant *ld* alleles. PCR primers (primer A: 5′ cagtctcagaagcaacagtg 3′; primer B: 5′ tctgacagaggtgagcaagg 3′) flanking a CA repeat at the *ld* locus were used for amplification reactions on DNA extracted from extraembryonic membranes. Cycling conditions were as follows: 2 minutes at 94°C, followed by 35 cycles of 94°C denaturing (30 seconds), 58°C annealing (30 seconds) and 72°C extending (1 minute). Reactions were resolved on a 10% polyacrylamide gel containing 1× TBE (90 mM Tris-borate, 20 mM EDTA).

Whole-mount in situ hybridizations

Pilot experiments were performed with the *fgf-4* riboprobe to optimize for consistent AER staining. We found that the standard Protease K permeabilization protocol (Wilkinson, 1992) often resulted in destruction of the AER structure, whereas detergent permeabilization (Rosen and Beddington, 1993) resulted in consistent and strong signals from the *fgf-4* riboprobe. As a result, all the AER staining in this study was done using detergent permeabilization, while Protease K was used to optimally stain other structures, such as limb mesoderm. After permeabilization, in situ hybridizations were performed as previously described (Riddle et al., 1993), except that 0.1% Tween 20 was used in the post-antibody washes.

Probes

For the *ld* isoform expression studies, probe I-III was constructed by subcloning the 1692 basepair *Xba*I/*Hin*dIII fragment from isoform I (Woychik et al., 1990b) into pBluescript (Stratagene). Probe IV is a 1568 basepair *Eco*RI/*Nae*I fragment from isoform IV (Jackson-Grusby et al., 1992) in pBluescript. Probe I-IV is a 1346 basepair *Stu*/*Spe* fragment from isoform I in pBluescript. The other probes were *fgf-4* (Hébert et al., 1990) (kindly provided by J. Hébert), *shh* (Echelard et al., 1993) (kindly provided by A. McMahon), *Hoxd-12* (kindly provided by A. Burke) and *Hoxd-9* (kindly provided by P. Chambon).

An *Evx1* cDNA fragment was generated by the polymerase chain reaction (PCR) using the following primers: 5′ gactgcaggatggacgtcgt

3′ and 5′ ttcattccctgcaggaaggac 3′. The 1140 basepair product was digested with *Pst*I and subcloned into pBluescript. The *fgf-8* cDNA was generated by PCR using the following primers: 5′ atggatcctg-cacttgctggttctctgc 3′ and 5′ atgaattcgcacaactagaaggcagctc 3′. The ~700 basepair product was digested with *Bam*HI/*Eco*RI and subcloned into pBluescript. The *Evx1* and *fgf-8* subclones were confirmed by partial sequencing using T3 and T7 sequencing primers.

Transgenic mice

A 6 kilobase *Bgl*II/*Bam*HI fragment, containing isoform IV 5′ flanking sequences, was subcloned upstream of the *lacZ* gene (Fields-Berry et al., 1992). This construct fused 65 amino acids of isoform IV with residue 7 of *lacZ*. Transgenic mice were generated by pronuclear injection of fertilized eggs and founders identified by Southern blotting (Sinn et al., 1987). Embryos were stained for *lacZ* expression as described previously (Cepko et al., 1993).

RESULTS

The four major transcripts from the *ld* locus are diagrammed in Fig. 1. Isoforms I-III are expressed coordinately, but their embryonic expression patterns are poorly understood since previous studies have been limited to the resolution of ribonuclease protection assays (Jackson-Grusby et al., 1992; Maas et al., 1994). An in situ hybridization study using an isoform IV probe has shown that this transcript is expressed in the AER of day 10.5 embryos, but other time points and organs were not analyzed (Jackson-Grusby et al., 1992). Therefore, we wished to examine in more detail the embryonic expression patterns of these two classes of transcripts by using whole-mount in situ hybridization. For these studies, three riboprobes were constructed, each specific to a different subset of *ld* transcripts (Fig. 1). The first probe (probe I-III) is derived from the 5′ exon common to isoforms I-III and therefore hybridizes to all three of these coordinately expressed transcripts. The second probe (probe IV) is derived from the 5′ exon of isoform IV and is specific for this transcript. Finally, the third probe (probe I-IV) consists of 3′ cDNA sequences that are present in all four transcripts. All the staining patterns described below

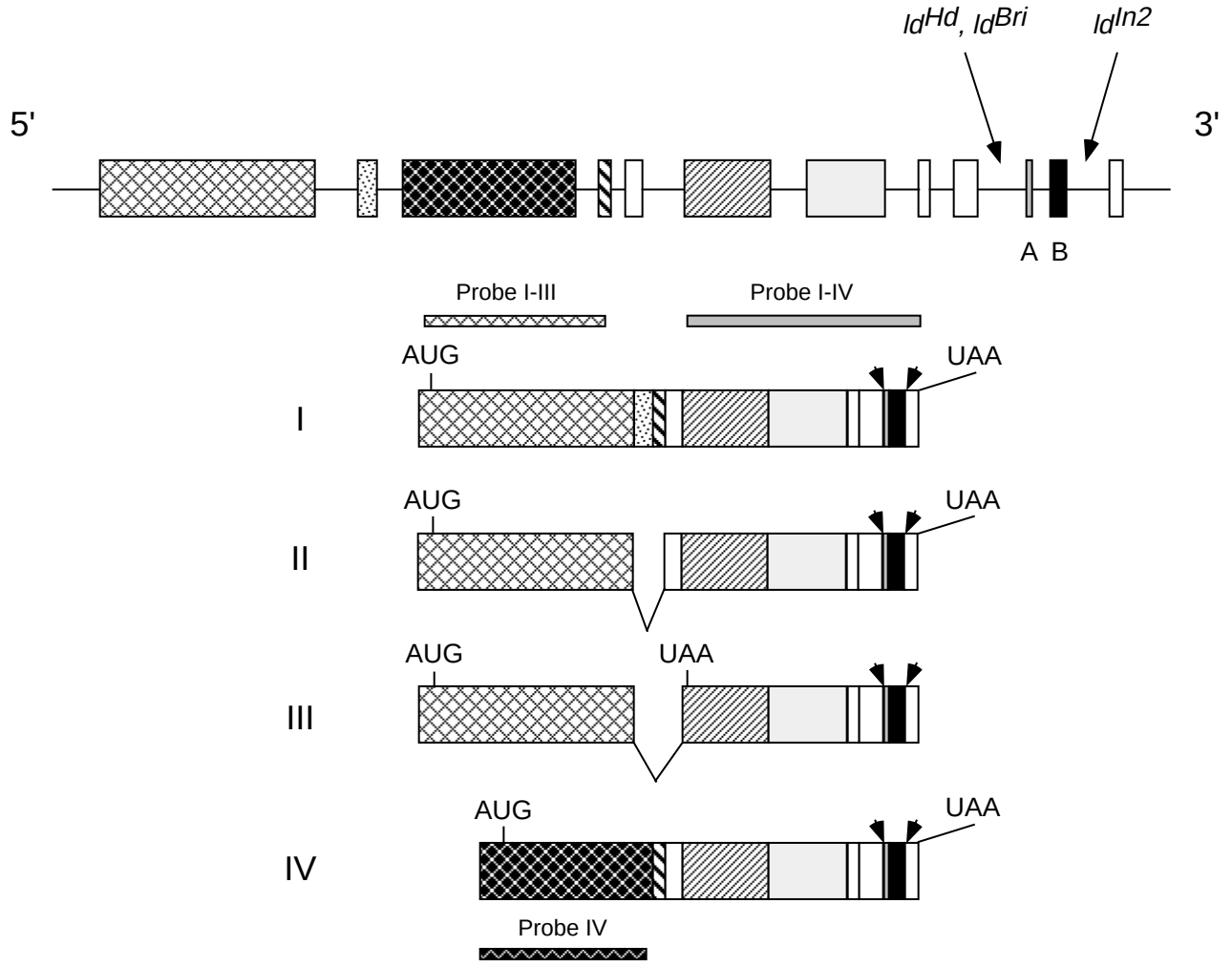

Fig. 1. Diagram of *ld* isoforms and in situ probes. On the top is a diagram of the *ld* genomic locus, with boxes representing exons. Not all the *ld* genomic sequences have been cloned and the actual exon/intron structure is likely to be more complicated. Introns (represented by horizontal lines) are not drawn to scale. Arrows and arrowheads indicate the positions of the ld^{TgHd}, ld^{TgBri} and ld^{In2} disruptions (Maas et al., 1990; Vogt et al., 1992). The four major *ld* transcripts, with positions of start and termination codons marked, are indicated below the genomic structure. Note that these mutations do not affect the coding sequence of isoform III, which terminates before the disruptions. The three in situ riboprobes are indicated by narrow bars.

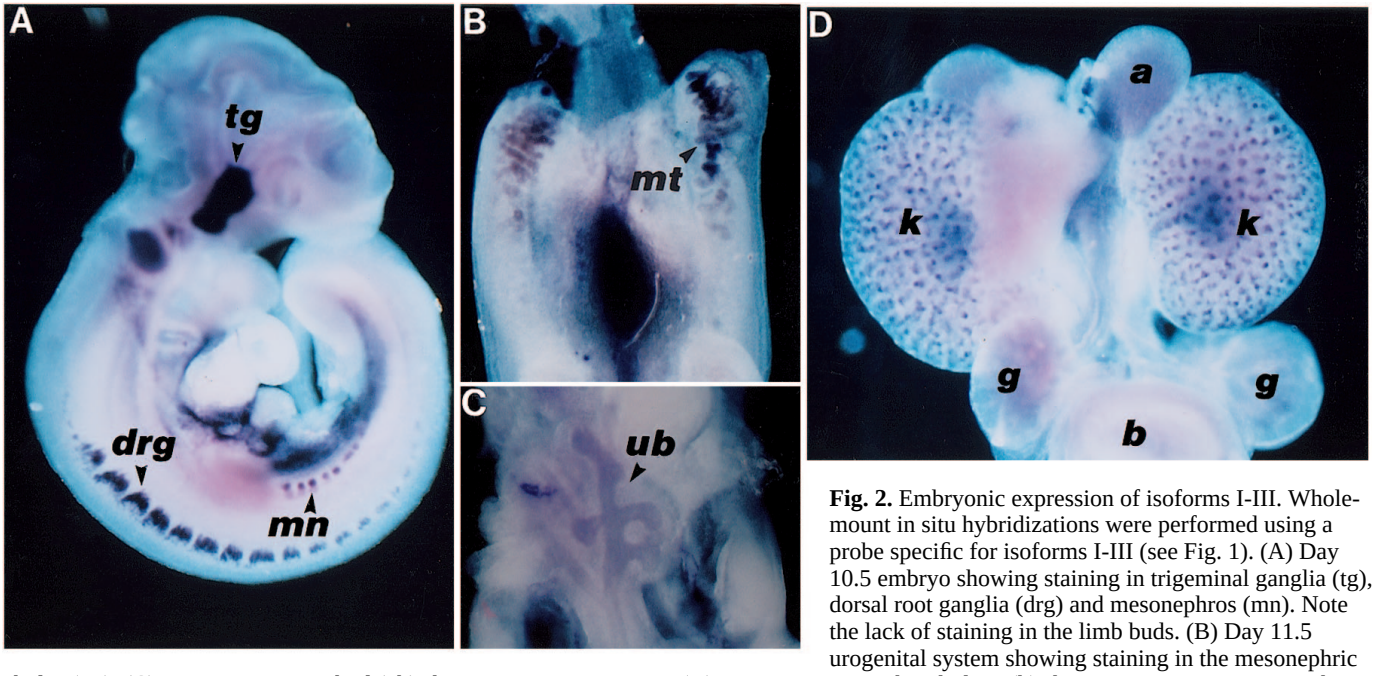

Fig. 2. Embryonic expression of isoforms I-III. Whole-mount in situ hybridizations were performed using a probe specific for isoforms I-III (see Fig. 1). (A) Day 10.5 embryo showing staining in trigeminal ganglia (tg), dorsal root ganglia (drg) and mesonephros (mn). Note the lack of staining in the limb buds. (B) Day 11.5 urogenital system showing staining in the mesonephric tubules (mt). (C) Day 11.5 ureteric bud (ub) showing positive staining. (D) Day 15.5 metanephric kidney (k) showing punctate staining. The staining in the renal pelvis is due to nonspecific staining, since it is observed with sense riboprobes. a, adrenal gland; b, bladder; g, gonads.

were obtained only with anti-sense riboprobes and not with control sense riboprobes.

Isoforms I-III are expressed in dorsal root ganglia, cranial ganglia and the developing kidney

We first detected expression of isoforms I-III starting in day 9.5 embryos. At this time, staining was observed in the trigeminal ganglia and the pronephros (not shown). The staining in the trigeminal ganglia intensifies at day 10.5, at which stage intense staining of dorsal root ganglia was also observed (Fig. 2A). Expression in these two structures was maintained until at least day 16.5, the latest embryonic stage examined (not shown). The identities of these structures were confirmed by serial sections of stained embryos (not shown). Significantly, no limb bud staining was evident at any stage examined (days 8.5 to 16.5), consistent with previous ribonuclease protection experiments (day 10.5 shown in Fig. 2A) (Jackson-Grusby et al., 1992). This result argues that isoforms I-III are not involved in the limb phenotype of *ld* mice.

Since *ld* mice display renal aplasia or hydronephrosis, we decided to explore further the expression of isoforms I-III in the developing kidney system. Staining was seen in the pronephros of day 9.5 embryos (not shown) and in the mesonephric tubules and mesonephric duct of day 10.5 embryos (Fig. 2A). For day 11.5 and older embryos, the urogenital system was dissected, fixed and prepared for whole-mount in situ hybridizations. We found this approach necessary for these older embryos because their relatively large size precludes access of the probe in intact embryos. At day 11.5, the ureteric bud has evaginated from the caudal end of the mesonephric duct and has established contact with the undifferentiated metanephric blastema (Kaufman, 1992). Shortly thereafter, the ureteric bud, under the influence of the metanephric blastema, starts to branch extensively. As the ureteric bud branches, it in turn induces differentiation of the metanephric mesenchyme, which by day 14.5 has begun to form the distal tubules, the proximal tubules, the loop of Henle and the glomeruli. The branchings of the ureteric bud differentiate into the collecting tubules.

In view of the critical inductive events that occur on embryonic day 11.5, it is striking that at this stage isoforms I-III are expressed in the mesonephric tubules, the mesonephric duct and throughout the ureteric bud, including its branchings (Fig. 2B,C). No significant expression was observed in the metanephric mesenchyme. By day 14.5 (not shown) and 15.5 (Fig. 2D), isoforms I-III are expressed in a punctate pattern in the metanephric kidney, reflecting the extensive branching of the ureteric bud derivatives. Sections of these older kidneys show that some mesenchymal cells also express isoforms I-III at these stages (not shown). These results suggest that isoforms I-III may play a role in early ureteric bud differentiation or outgrowth. Interestingly, deficient outgrowth of the ureteric bud is likely to be the defect underlying renal agenesis in ld^J mice (Maas et al., 1994).

Isoform IV is expressed in the AER, somites, notochord and developing kidney

The most prominent site of isoform IV expression is in the AER of day 9.5 (not shown), 10.5 (Fig. 3A,B) and 11.5 embryos (not shown). The staining covers most of the length of the AER (Fig. 3B) and therefore is significantly more extensive than that of *fgf-4* (see below), which shows a posterior bias in its AER expression (Niswander and Martin, 1992). In addition, isoform IV expression is first evident in the ectoderm of day-9.5 limbs (not shown) and is thus present before the onset of *fgf-4* expression, which begins at day ~10.0-10.5 (Niswander and Martin, 1992). Punctate limb mesenchyme staining is seen in embryos that have been perme-

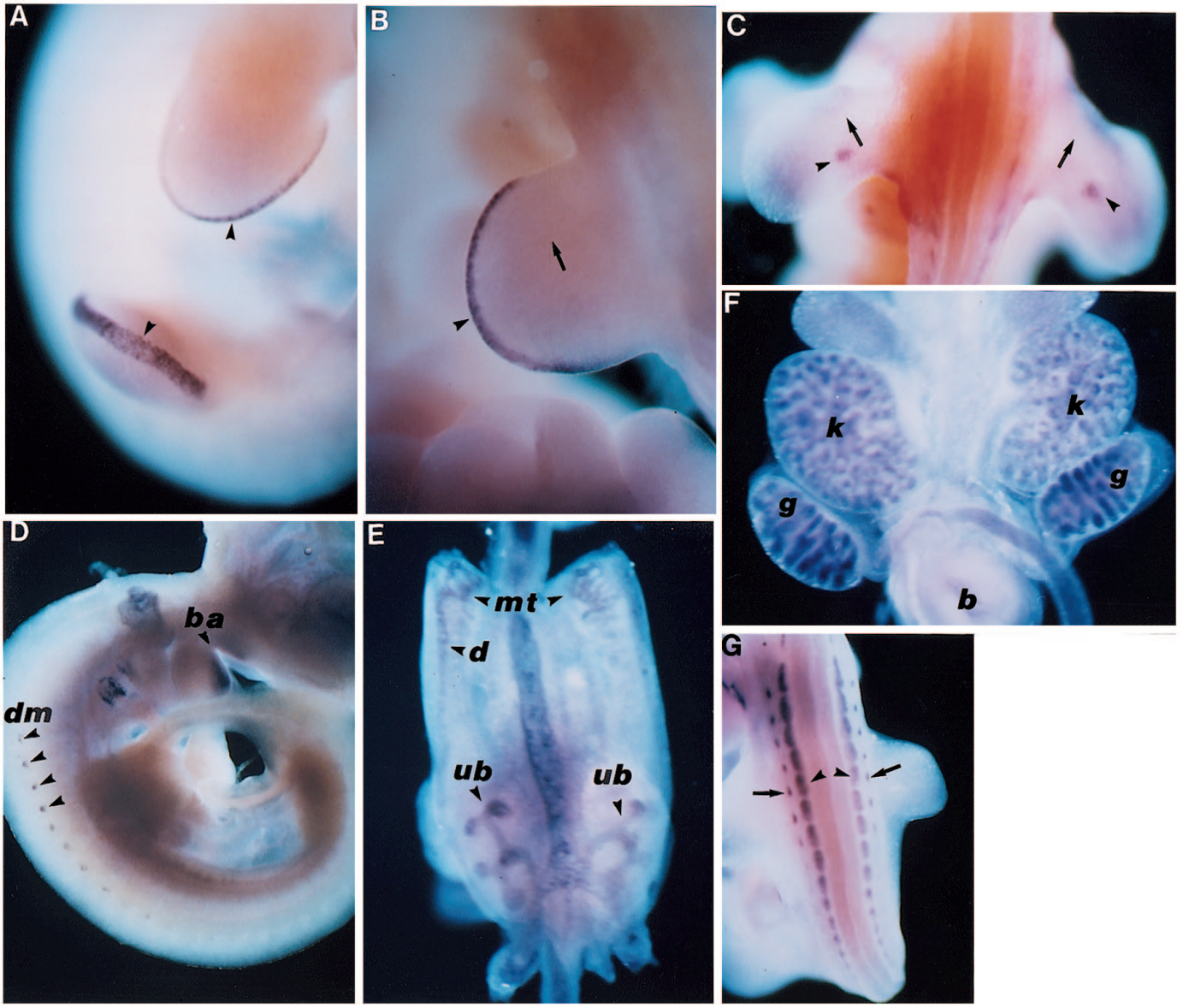

Fig. 3. Embryonic expression of isoform IV. Whole-mount in situ hybridizations were performed using a probe (see Fig. 1) specific for isoform IV (A-F) or isoforms I-IV (G). The samples in (A) and (B) were permeabilized with detergent; the others were permeabilized with Protease K. (A) Day 10.5 embryo showing AER staining (arrowheads) in both the forelimbs (top limb) and hindlimbs. (B) A dorsal view of a day 10.5 hindlimb to show the extent of AER staining. Anterior is in the direction indicated by the arrow. (C) Dorsal view of day 11.5 hindlimb buds, showing discrete staining (arrowheads) in the posterior mesoderm. Arrows indicate anterior direction. (D) Day 10.5 embryo showing staining in the dermamyotomes (dm, arowheads) and branchial arches (ba). (E) Day 11.5 urogenital system, showing staining in the mesonephric tubules (mt), mesonephric duct (d) and branching ureteric bud (ub). (F) Day 15.5 urogenital system showing punctate staining in the metanephric kidney (k) and gonads (g). b, bladder. (G) Day 10.5 embryo showing staining (isoforms I-IV) in dorsal root ganglia (arrowheads) and dermamyotomes (arrows).

abilized with protease K (Fig. 3C). This discrete mesenchymal staining is in the posterior portion of both fore- and hindlimbs and appears to be anterior to the polarizing region marked by *shh* expression (not shown). At present we do not know the significance of this mesenchymal staining in the limb bud.

Isoform IV is also expressed in the dermamyotomes of day 9.5 (not shown) and 10.5 embryos, most intensely in the anterior somites, which are at a more advanced developmental stage (Fig. 3D). This transcript is also expressed in the branchial arches (Fig. 3D). Paraffin sections of stained embryos show that isoform IV is also expressed throughout the length of the notochord (not shown).

Like isoforms I-III, isoform IV is also expressed throughout kidney development. It is first expressed in the pronephros of day-9.5 embryos and in both the mesonephric tubules and the mesonephric duct of day-10.5 embryos (not shown). As with the isoform I-III probe, we examined the expression of isoform IV in later kidney development by staining dissected urogenital systems. The staining patterns are very similar to those obtained with the isoform I-III probe. Isoform IV is present in

the mesonephric tubules, the mesonephric duct and the ureteric bud of day 11.5 embryos (Fig. 3E). Later stage metanephric kidneys show the same punctate staining (reflecting ureteric bud derivatives) seen with the isoform I-III probe (Fig. 3F). In addition, the embryonic gonads express isoform IV, but not I-III (compare Fig. 3F to 2D).

A carboxyl-terminal probe combines the staining patterns of isoforms I-IV

Isoforms I-IV share common 3′ sequences, suggesting a structural relationship in which there is a relatively constant carboxyl-terminal portion and relatively variable amino-terminal portions among the formins. As expected, when embryos were hybridized with probe I-IV (derived from the 3′ or constant region of the *ld* gene), a composite staining pattern was obtained that combined the expression patterns of isoforms I-III (Fig. 2) and isoform IV (Fig. 3). Staining was seen in the limb bud, somites, dorsal root ganglia, notochord, trigeminal ganglia and developing kidney (Fig. 3G shows staining in dorsal root ganglia and somites).

Identification of isoform IV regulatory sequences

Since the expression pattern of isoform IV differs significantly from that of isoforms I-III, we thought that the expression of isoform IV may be controlled by regulatory sequences upstream of its 5′ most exon. To test this possibility, we subcloned a 6 kilobase *Bgl*II/*Bam*HI fragment from the 5′ flanking region upstream of the first exon of isoform IV. This fragment encoded 65 amino acids of the first exon and was fused in-frame with the reporter gene *lacZ* (Fig. 4A). Five lines of transgenic mice were generated with this construct and transgenic embryos were stained for *lacZ* expression. One of these lines did not express, while 4 lines showed expression in the embryonic limb bud (Fig. 4B-E). There was some variability in the overall staining patterns among the four expressing lines, but all four lines showed limb ectoderm staining, with highest levels restricted to the AER. These results identify distinct regulatory sequences that control the expression of isoform IV.

ld limb buds contain an abnormally organized and incompletely differentiated AER

Previous histological studies showed that *ld* limb buds contain an AER with cuboidal cells that resemble non-AER ectoderm, in contrast to wild-type AER cells which are columnar and distinct from surrounding ectoderm (Zeller et al., 1989). In addition, the mutant AERs are non-uniform, consisting of patches of thickened AER interspersed with patches of flattened AER. In order to assess the differentiation state of *ld* AERs, we stained wild-type and mutant embryos with a series of previously characterized AER markers. For precise comparisons between wild-type and mutant embryos, we used primarily embryos from homozygous ld^{In2} females mated to heterozygous ld^{In2} males. We also repeated the experiments using mice bearing a different allele, ld^{TgBri}. Analyses of mice bearing either allele were equivalent. This mating scheme allowed the comparison of homozygous mutants to their phenotypically wild-type (heterozygous) littermates.

Most significantly, we found no detectable expression of *fgf-4* in the limb ectoderm of ld^{TgBri} (not shown) and ld^{In2} homozygous embryos (Fig. 5A, left embryo; also compare Fig. 6A with 6B) even when the embryos were intentionally overstained (Fig. 5A), although its expression in other sites (such as myotomes) was unaffected. In heterozygous littermates, *fgf-4*

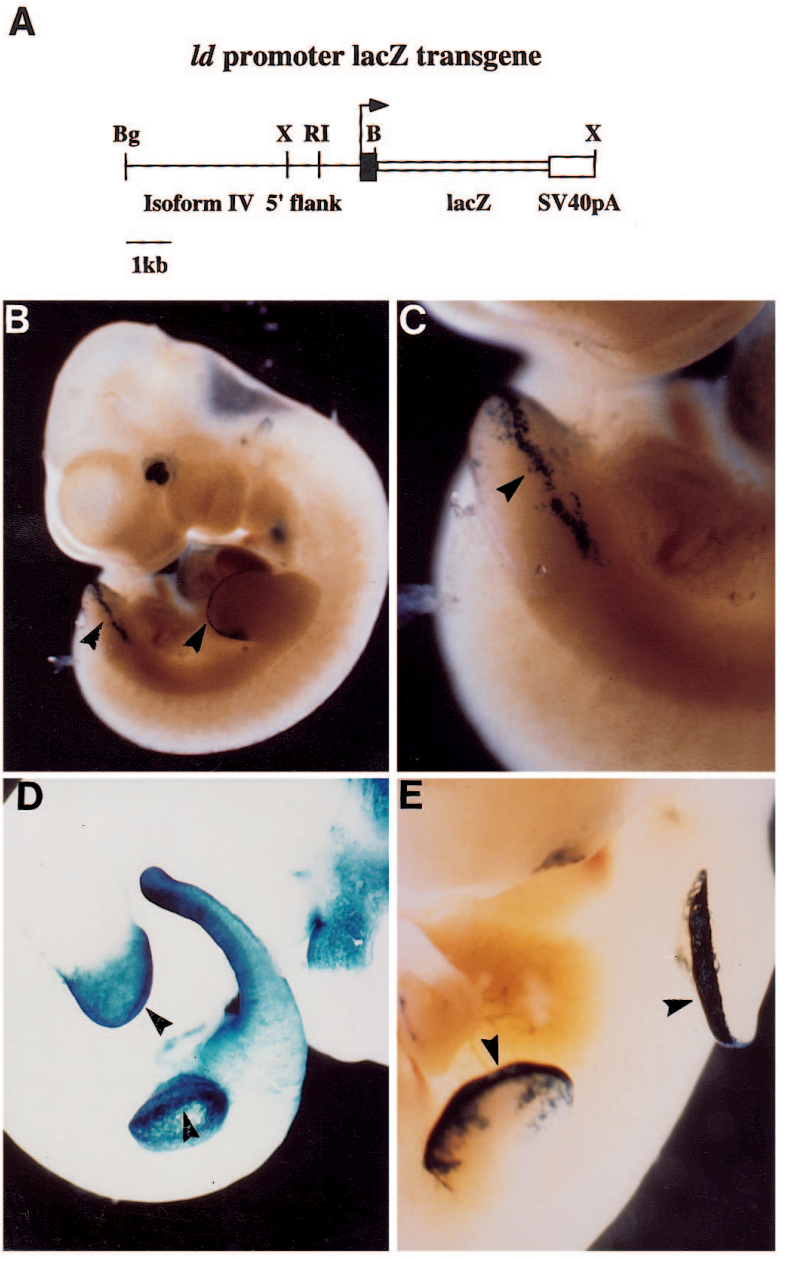

Fig. 4. Identification of isoform IV regulatory sequences. (A) Schematic of the isoform IV-*lacZ* transgene. (B) Day 10.5 embryo from WA line, showing *lacZ* expression in the AER (arrowheads). (C) Higher magnification of hindlimb in (B), showing intense staining in the AER (arrowhead). (D) Day 10.5 embryo from WA-1 line, showing *lacZ* expression in the limb ectoderm, with highest levels in the AER (arrowheads). (E) Day 12.5 embryo from WA-4 line, showing *lacZ* expression the AER (arrowheads).

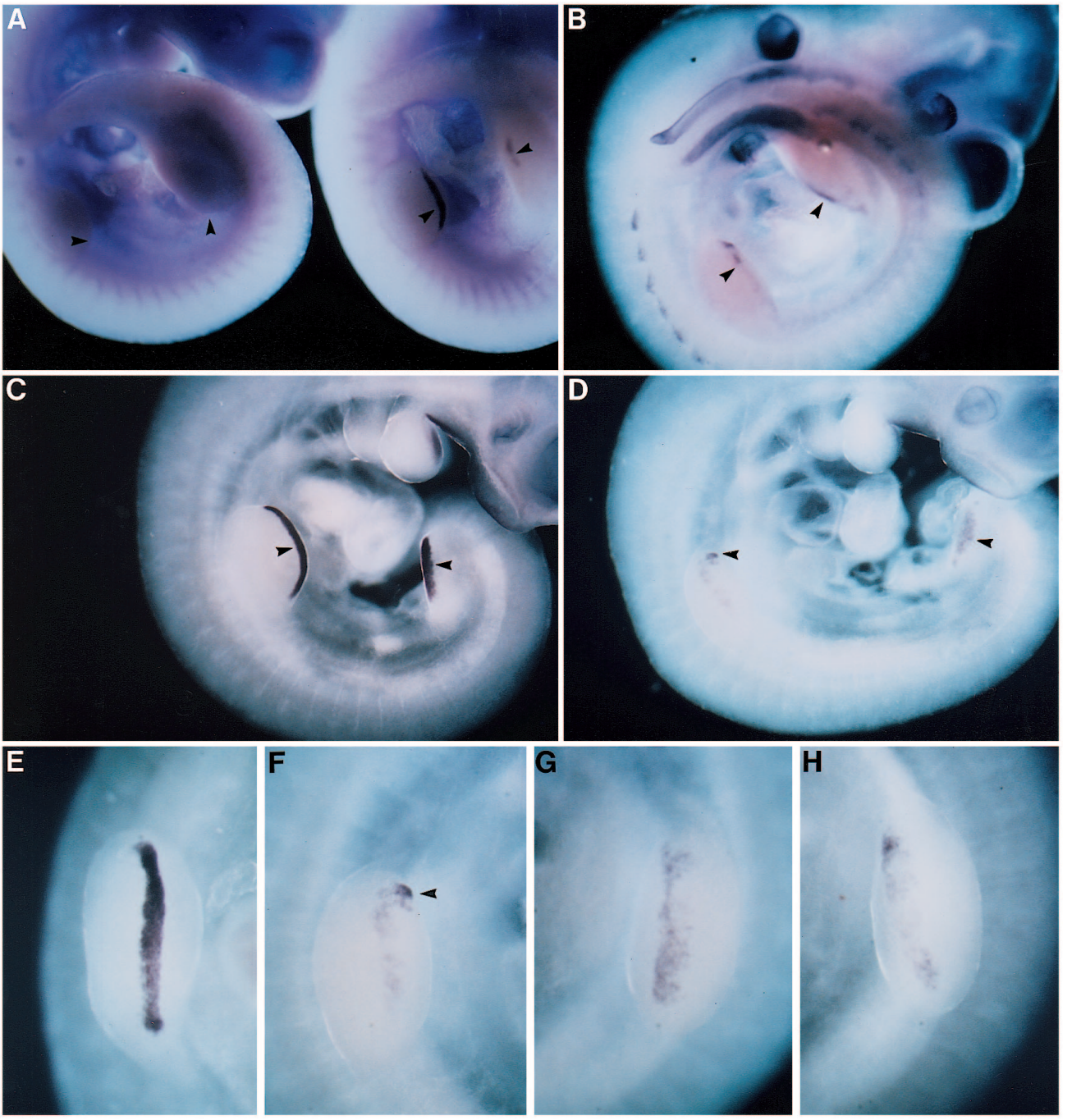

Fig. 5. Expression of AER markers in ld^{In2} and ld^{TgBri} embryos. Whole-mount in situ hybridizations were performed on day 10.5 embryos. (A) Two day 10.5 littermates hybridized to *fgf-4* riboprobe. The homozygous ld^{In2} mutant (left) shows no AER expression (arrowheads), while the heterozygous littermate (right) shows intense expression in the forelimb AER (arrowhead) and lower expression in the hindlimb AER (arrowhead). The embryos have been intentionally overdeveloped to detect any weak signals in the mutant. Note normal expression of *fgf-4* in the myotomes of the mutant (left) embryo. (B) Day10.5 ld^{In2} homozygote showing *ld* isoform IV expression in the forelimb and hindlimb AER (arrowheads). Note the irregular pattern of the forelimb AER staining. (C,D) Day10.5 littermates hybridized to *fgf-8* riboprobe. (C) An ld^{TgBri} heterozygote showing intense AER staining (arrowheads). (D) An ld^{TgBri} homozygote showing much more faint AER staining (arrowheads). Note the dorsoventral spreading (arrowhead) in the anterior AER of the forelimb. (E-H) Representative forelimbs stained with an *fgf-8* riboprobe. (E) A right forelimb from an ld^{TgBri} heterozygote; (F) a right forelimb from an ld^{In2} homozygote; (G) a left forelimb from an ld^{In2} homozygote; (H) a left forelimb from an ld^{TgBri} homozygote. Note the dorsoventral spreading in the anterior AER (arrowhead, F) and the discontinuity of the AER (H). Also note the variability in staining patterns among F, G and H.

is expressed intensely in the central and posterior AER beginning slightly before day 10.5 (Fig. 5A, right embryo) and fading substantially by day 11.5 (not shown). Limb buds of ld^{In2} embryos showed no *fgf-4* staining at days 9.5, 10.0, 10.5, or 11.5 (day 10.5 shown in Fig. 5A). Twenty day 10.5 ld^{In2} homozygotes were examined and at least five of each of the

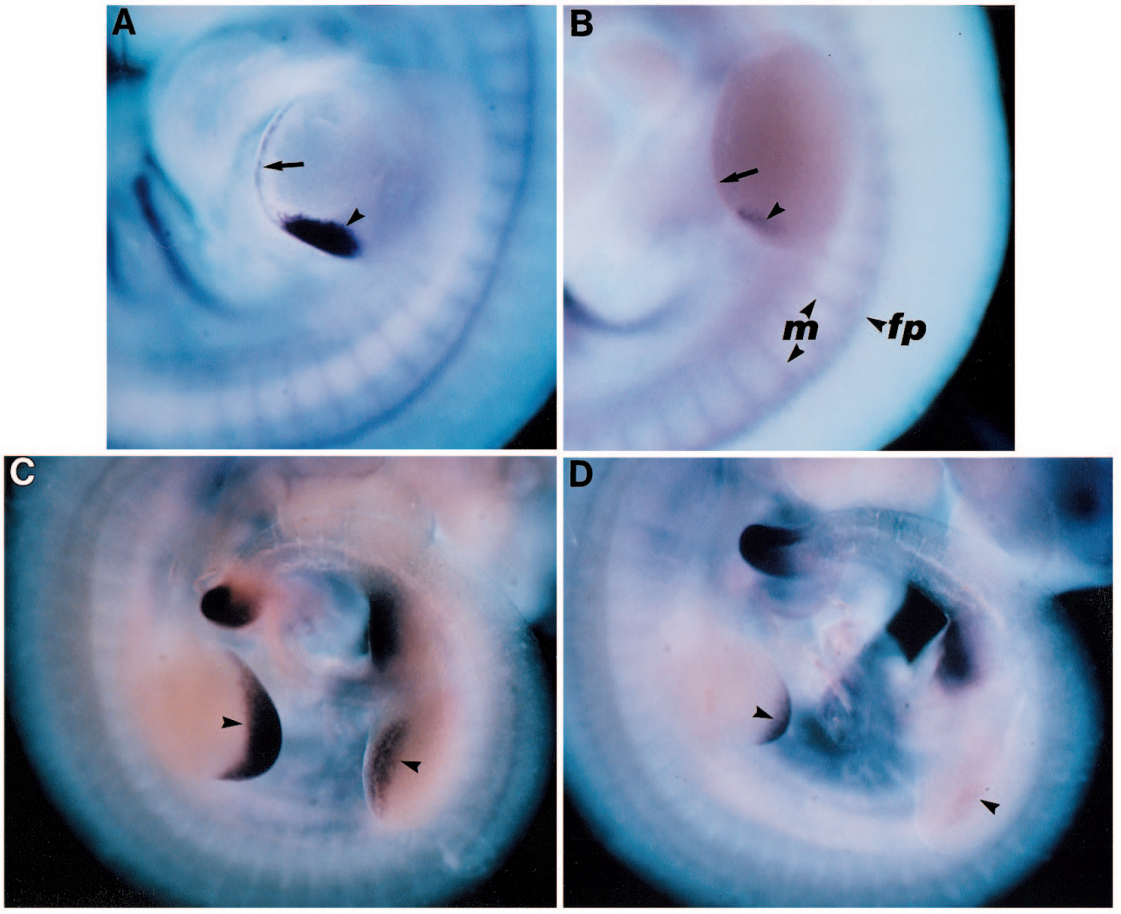

Fig. 6. *Shh* and *Evx1* expression in *ld* embryos. (A,B) Forelimbs hybridized to *shh* and *fgf-4* riboprobes simultaneously. (A) Wild-type embryo showing *shh* expression in the posterior limb mesoderm (arrowhead) and *fgf-4* expression in the AER (arrow). (B) ld^{In2} homozygote showing faint *shh* expression in a small region of posterior mesoderm (arrowhead) and no *fgf-4* staining in the AER (arrow). Note that there is normal *shh* expression in the floorplate (fp) and normal *fgf-4* expression in the myotomes (m). (C,D) Day 10.5 embryos (littermates) hybridized with *Evx1* riboprobe. (C) ld^{In2} heterozygote showing intense *Evx1* expression in the distal mesoderm (arrowheads) underlying the AER. (D) ld^{In2} homozygote showing reduced expression in the forelimb and hindlimb (arrowheads).

other stages were examined. Ten ld^{Bri} homozygotes were examined at day 10.5, but not at other embryonic stages.

We were initially concerned that the complete lack of *fgf-4* staining might be due to the absence of posterior AER cells in mutant embryos. However, the AERs of mutant embryos were found to express a number of AER markers, including *bmp4*, *Msx2* (both not shown), *ld* isoform IV (Fig. 5B) and *fgf-8* (Fig. 5D,F,G,H). These positive markers allowed visualization of *ld* AERs and revealed the presence of posterior AER cells. Consistent with previous histological studies, the AERs of mutant embryos were patchy, such that the ridge no longer formed the uniform and continuous strip seen in control limbs (compare Fig. 5E with 5F-H; also 5B with 3A,B). In addition, the cells in the *ld* mutant ridges tended to spread more dorsoventrally than their wild-type counterparts; this spreading was observed more frequently in the anterior part of the AER (Fig. 5D,F). In both the ld^{In2} and the ld^{TgBri} lines, this patchiness and dorsoventral spreading of the mutant AER was variable from embryo to embryo (Fig 5F-H). It should be noted that *fgf-8* staining in the *ld* AERs was much weaker than in heterozygous littermates. The observation that *ld* limb buds produce *fgf-8* is interesting, because the onset of *fgf-8* expression is markedly earlier than *fgf-4* (Crossley and Martin, 1995). These results indicate that although *ld* limb buds lack *fgf-4* expression, they contain at least one FGF in the early stages of limb development.

ld limb buds have reduced expression of mesodermal markers

Morphological studies showed that *ld* limb buds, in addition to having an AER defect, have a shortened anteroposterior axis (Zeller et al., 1989). This reduction is first apparent at day 10.5, when the anteroposterior width of mutant limb buds is almost 20% shorter than wild-type littermates. By day 11.5, this difference has increased to 30-40%. To examine the anteroposterior axis, we stained *ld* embryos with a number of mesodermal markers. We were particularly interested in the expression of *shh* and *Evx1*, since the expression of both these genes is thought to be regulated by *fgf-4* (Niswander and Martin, 1993; Laufer et al., 1994; Niswander et al., 1994). The expression of *shh* was found to be dramatically reduced in day 10.5 (Fig. 6A,B) and 11.5 limb buds (not shown), in both its level and domain of expression. Similarly, expression of the homeodomain-containing gene *Evx1* in *ld* limb buds was reduced,

but still detectable (Fig. 6C,D), suggesting that low levels of *Evx1* can be produced in the absence of *fgf-4*.

We next examined the expression of *Hoxd* cluster genes. *Hoxd-12* is expressed in the posterior mesoderm of day 10.5 and day 11.5 *ld* limb buds but, like *shh*, its level and domain of expression are significantly reduced (compare Fig. 7A,C with B,D). Even accounting for the shortened anteroposterior axis of the mutant limb buds, the domain of *Hoxd-12* expression occupies proportionately less space along the anteroposterior axis in mutant limb buds than in wild-type limb buds. This observation raises the possibility that posterior mesoderm may be specifically reduced in *ld* mutant limbs. In contrast, *Hoxd-9* is expressed throughout the limb mesoderm, in both wild-type and *ld* mutant limbs (Fig. 7E,F).

DISCUSSION

Differential expression of *ld* transcripts in embryogenesis

Our in situ results show that *ld* transcripts I-III have a very different embryonic expression pattern compared to transcript IV. While both classes are expressed similarly in the developing kidney, transcripts I-III are uniquely expressed in dorsal root ganglia and cranial ganglia. Since the coding sequences of isoforms I, II and IV are known to be disrupted in the ld^{TgHd}, ld^{TgBri} and ld^{In2} mutations (Maas et al., 1990; Vogt et al., 1992), these expression patterns lead to the question of whether *ld* mice have other subtle defects, such as sensory perception, which have thus far gone undetected. Our gross examination of the ld^{TgBri} and ld^{In2} mice have revealed no such defects, but more detailed and sensitive studies may be required.

All four isoforms are expressed during the three stages of kidney development: the pronephros, the mesonephros and the metanephros. Their expression in the ureteric bud is particularly interesting because the renal aplasia seen in ld^{J} mice is thought to result from delayed or nonexistent outgrowth of the ureteric bud (Maas et al., 1994). Because reciprocal inductive interactions occur between the ureteric bud and the metanephric mesenchyme (Saxen, 1987), this defect in ureteric bud outgrowth may reflect a primary defect in either the ureteric bud itself or the metanephric mesenchyme. However, the metanephric mesenchyme of *ld* embryos has been shown to be competent in responding to inducers (Maas et al., 1994), suggesting that the renal defect in *ld* mice may be intrinsic to

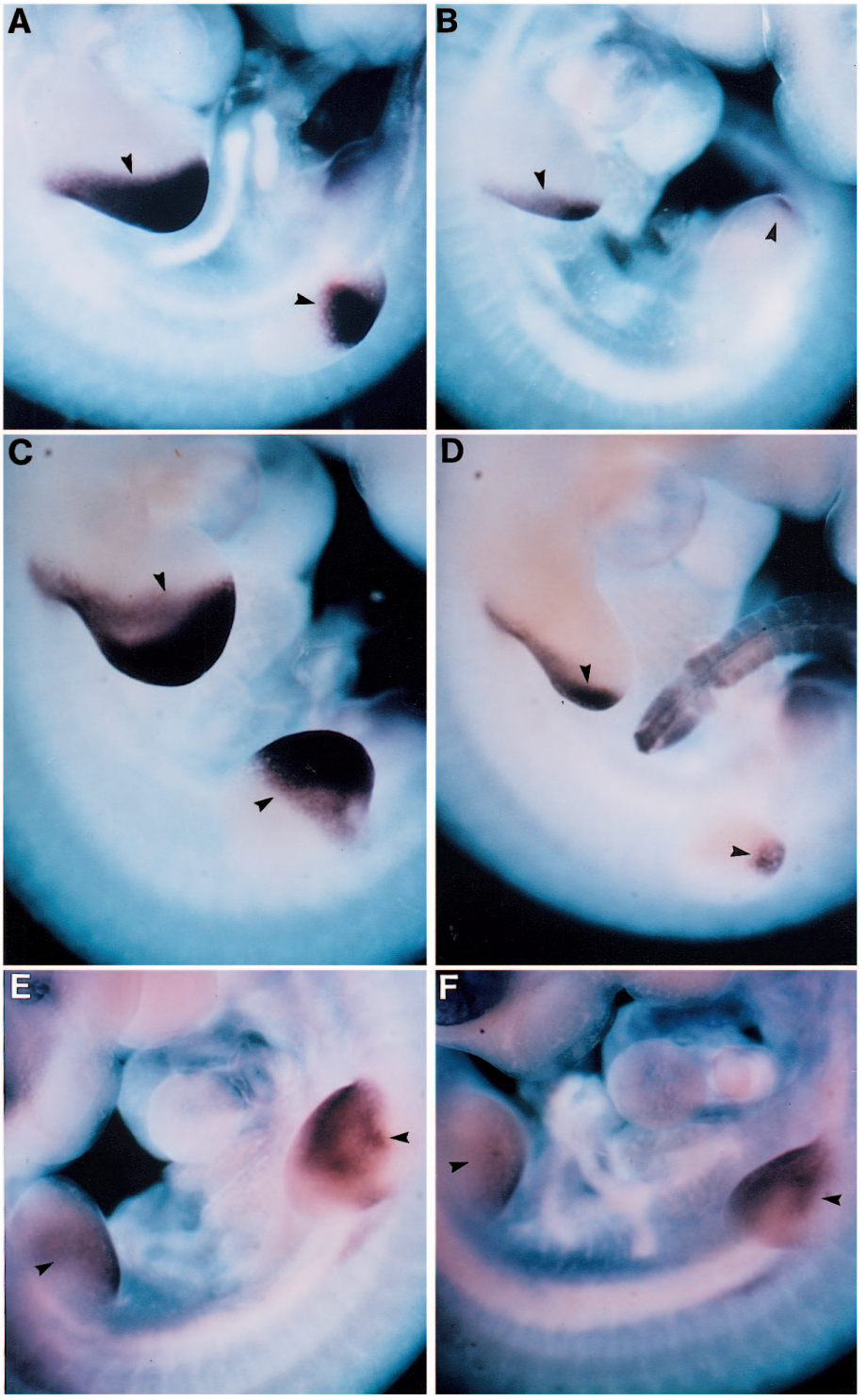

Fig. 7. *Hoxd-12* and *Hoxd-9* expression in *ld* embryos. (A-D) Embryos hybridized to *Hoxd-12*. (A) Day 10.5 ld^{In2} heterozygote; (B) day 10.5 ld^{In2} homozygote. A and B are littermates. Note the reduction in the level and domain of expression in the homozygote. (C) Day 11.5 ld^{In2} heterozygote; (D) day 11.5 ld^{In2} homozygote. C and D are littermates. Note the reduced anteroposterior width of the homozygous limbs compared to the heterozygous limbs. (E) Day 10.5 ld^{In2} heterozygote hybridized to *Hoxd-9* riboprobe. (F) Day 10.5 ld^{In2} homozygote hybridized to *Hoxd-9* riboprobe. E and F are littermates.

the ureteric bud. Thus, all four isoforms may play a role in promoting ureteric bud outgrowth.

In contrast to the renal structures, isoform IV is specifically expressed in the limb AER, the structure in which the limb defect can first be discerned. We have identified regulatory sequences, located upstream of the first exon of isoform IV and 3′ of the first exon of isoforms I-III, that control the differential expression of isoform IV. We do not know the precise distance between these two exons, but genomic mapping experiments indicate a minimal distance of ~20 kb (C. Wang and P.L., unpublished results). Although the expression of isoform IV in the AER suggests a role in the *ld* limb phenotype, recent experiments show that mice containing a targeted disruption of only isoform IV have morphologically normal limbs (T. Wynshaw-Boris et al., unpublished data). The lack of a limb phenotype in these mice suggests that the function of isoform IV in the limb is likely to be redundant with other *ld* isoforms which have not been fully characterized. At least two other *ld* transcripts are expressed in the limb ectoderm and these are currently being characterized (C. Wang and P. L., unpublished results). Interestingly, isoform IV-deficient mice have a low incidence of renal aplasia. Their incidence of renal aplasia is lower than in ld^{TgHd} or ld^{TgBri}, and it is possible that the additional disruption of isoforms I-III in the latter mice (Maas et al., 1990; Vogt et al., 1992) contributes to their stronger phenotype. Alternatively, these differences might be due to strain background effects rather than to differences inherent to the alleles.

It is instructive to compare the differential expression of the murine *ld* isoforms with the expression of the *ld* gene in the chick. In the chick, immunohistochemical studies (Trumpp et al., 1992) using antibodies directed to carboxyl epitopes show an expression pattern similar to the pattern that we see in the mouse embryo using probe I-IV. Thus far only one chick *ld* isoform, corresponding to murine isoform IV, has been identified. It remains to be seen whether multiple isoforms with differential expression also exist in the chick, or whether the chick has only one *ld* isoform with a broader expression pattern that encompasses the expression domains of isoforms I-IV in the mouse.

Partial AER defect in *ld* limb buds and the role of *fgf-4* in limb outgrowth

Our results provide a molecular framework for understanding the AER defect in *ld* limb buds. Although the cells in the AER of *ld* limb buds are incompletely differentiated (Zeller et al., 1989), we find that they do express several AER-specific markers, including *ld* isoform IV and *fgf-8*. The use of these markers allowed us to visualize easily the intact AER of *ld* embryos and therefore to observe the extensive variability of the AER structure in different limbs. The AERs of mutant embryos are often noncontinuous and show dorsoventral spreading of cells. The AER is required for proper proximodistal outgrowth, since AER removal results in truncated limbs that lack distal elements (Saunders, 1948). *ld* limbs, however, do not show such extensive proximodistal defects (Kleinebrecht et al., 1982). Although *ld* limbs are shorter than wild-type limbs and show a reduction in the number of digits, they are not truncated but instead contain the full spectrum of skeletal elements. Taken together, these observations indicate that the *ld* AER probably retains significant AER function.

The absence of *fgf-4* expression in *ld* limbs deserves special consideration. FGF4, when applied to limb buds in which the ridge has been removed, is capable of both maintaining polarizing activity and promoting full proximodistal outgrowth (Niswander et al., 1993; Vogel and Tickle, 1993). It is therefore a good candidate for the AER signal. *ld* limb buds do not express detectable *fgf-4* and yet form the most distal skeletal structures (digits), implying that *fgf-4*, while capable of promoting limb outgrowth under experimental conditions, is not essential for this process in normal limb development. This observation is particularly interesting because the question of whether *fgf-4* is required for limb outgrowth has been difficult to approach. Mice containing a null mutation in *fgf-4* die shortly after uterine implantation and show poor proliferation of the inner cell mass (Feldman et al., 1995). Due to this early embryonic lethality, the role of *fgf-4* in limb development could not be assessed using these mice. In *ld* mice, however, the disruption of *fgf-4* expression is specific for the AER and therefore analysis of *ld* embryos allows us to conclude that *fgf-4* is not essential for formation of distal limb structures. We cannot rule out the possibility that very low levels of *fgf-4* expression persist in *ld* limb buds and are sufficient for distal limb outgrowth.

One explanation for digit formation despite the *fgf-4* deficit might be that multiple *fgf* genes play redundant roles in limb development. Other *fgf* family members, such as *fgf-2* and *fgf-8*, may have similar proliferative functions in the limb, thereby mitigating the lack of *fgf-4* expression in *ld* limb buds. *Fgf-8* is indeed expressed in *ld* limb buds, although at much lower levels than in wild-type AERs. Since *fgf-8* is expressed earlier than *fgf-4* (Crossley and Martin, 1995), *ld* limbs may contain sufficient FGF activity during most of limb development to avoid major proximodistal defects. We would like to know if *ld* limb buds produce *fgf-2*, another candidate for the AER signal. Unfortunately, so far we have been unsuccessful in detecting *fgf-2* expression in mouse embryos using either in situ hybridization or ribonuclease protection assays, perhaps due to the low levels of *fgf-2* transcripts.

An alternative explanation is that the various *fgf* family members, although having similar proliferative actions when applied exogenously to limb buds, may actually play distinct roles during limb development. For example, *fgf-4*, because it is expressed in the posterior AER, may be primarily required for maintaining polarizing activity (Niswander et al., 1993; Vogel and Tickle, 1993) rather than for promoting distal outgrowth. The other *fgf* family members, such as *fgf-8*, may play more direct roles in maintaining proximodistal outgrowth. The reduction of *shh* in *ld* limb buds is consistent with this model.

Anteroposterior defects in *ld* limbs

Beginning at day 10.5, the limb buds of *ld* embryos show a shortened anteroposterior axis (Zeller et al., 1989). Skeletal analyses show that the hindlimbs of ld^{J} mice lack the most posterior digits (the forelimb defect, however, is more variable and is not strictly postaxial) (Kleinebrecht et al., 1982). Our in situ hybridization results indicate that the expression of *Hoxd-12*, a marker for posterior limb mesoderm, is greatly reduced in *ld* limb buds. Thus a defect in posterior limb mesenchymal outgrowth may account for the reduced anteroposterior axis. One possibility is that the reduced posterior mesenchymal

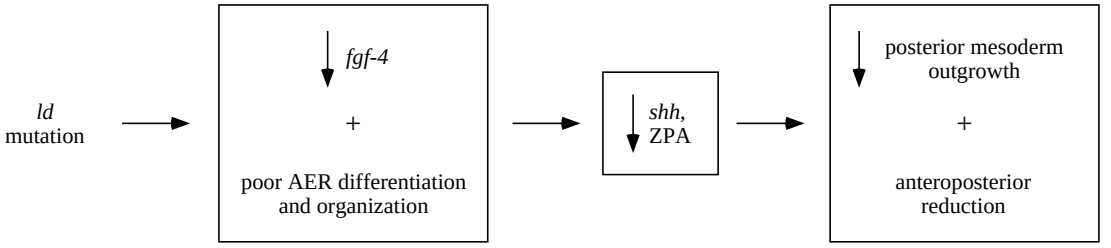

Fig. 8. A model for formin action. Our model proposes that formins are required for proper AER differentiation and function upstream of *fgf-4* and *shh*. In the absence of formin function, the AER is poorly differentiated and *fgf-4* is not expressed. This loss of *fgf-4* expression leads secondarily to a decrease in *shh* expression and polarizing activity. This decrease in polarizing activity results in reduced posterior limb mesoderm outgrowth, accounting for the anteroposterior defects seen in *ld* limbs. In this model, we have emphasized the role of formins expressed within the AER. However, it should be noted that the lower levels of formin isoform IV expression in posterior limb mesenchyme may also affect differentiation of the AER, due to reciprocal ectoderm-mesoderm interactions in the limb bud.

outgrowth is a direct consequence of the loss of *fgf-4*, which is normally expressed in the overlying posterior AER.

Alternatively, we suggest that reduction of *shh* expression and polarizing activity may be responsible for the posterior defect of *ld* limbs. Since *shh* is thought to mediate the polarizing activity of the ZPA (Riddle et al., 1993; Chang et al., 1994), *ld* limb buds probably have greatly reduced polarizing activity. The grafting of polarizing tissue into anterior chick limb mesoderm causes outgrowth and increased proliferation at the site of the graft (Saunders and Gasseling, 1968), suggesting that the ZPA may normally promote posterior mesenchymal outgrowth. Several lines of evidence support the view that reduction of polarizing activity leads to loss of posterior digits. First, when limiting amounts of polarizing tissue are grafted into host chick limb buds, the most posterior digits are not duplicated (instead of a full **4**-**3**-**2** duplication, only digits **3**-**2** or **2** are duplicated) (Tickle, 1981). Second, excision of the ZPA from early stage chick limb buds results in loss of posterior digits (Fallon and Crosby, 1975). Third, limb buds lacking *wnt-7a* expression show a reduction in *shh* expression and develop into limbs lacking posterior digits (Parr and McMahon, 1995; Yang and Niswander, 1995). Implantation of *shh*-expressing cells can rescue the posterior defect in such limb buds (Yang and Niswander, 1995).

The role of formins in limb morphogenesis

Previous immunohistochemical studies showed that chick formins are expressed in the posterior limb mesoderm, possibly in the region of the ZPA (Trumpp et al., 1992). Furthermore, chick formin is expressed in the notochord and floor plate, tissues that are known to contain polarizing activity. These observations raised the possibility that formins may be activated in response to polarizing signals. This idea, however, is inconsistent with the reduced *shh* expression seen in *ld* limb buds, which argues that formins function upstream of the polarizing region. Conversely, we think it is unlikely that formins are required for establishing or maintaining polarizing activity per se because *shh* expression in the notochord and floor plate of *ld* embryos is unaffected (Fig. 6B and Chan et al., unpublished results).

Our results therefore suggest that formins function early in limb patterning (Fig. 8). Isoform IV expression can be detected in the ectoderm of day 9.5 forelimbs and hindlimbs, as soon as the limb buds become distinct swellings on the flank. This onset of expression is earlier than that of both *shh* and *fgf-4*. We suggest that formins function upstream of *fgf-4* and are required for its expression. The loss of *fgf-4* expression in *ld* AERs may secondarily lead to a large reduction in *shh* production, since the expression patterns of these two genes are mutually linked (Laufer et al., 1994; Niswander et al., 1994; Yang and Niswander, 1995). This reduction of *shh* expression and polarizing activity may cause or contribute to defective posterior mesenchymal outgrowth, thereby leading to the anteroposterior abnormality of *ld* limbs.

We are grateful to A. Burke, P. Chambon, J. Hébert, G. Martin and A. McMahon for providing probes. We thank members of the Leder laboratory for helpful suggestions throughout this project.

REFERENCES

Cepko, C., Ryder, E. F., Austin, C. P., Walsh, C. and Fekete, D. (1993). Lineage analysis using retroviral vectors. *Methods in Enzymology* **225**, 933-960.

Chang, D. T., Lopez, A., Kessler, D. P. v., Chiang, C., Simandl, B. K., Zhao, R., Seldin, M. F., Fallon, J. F. and Beachy, P. A. (1994). Products, genetic linkage and limb patterning activity of a murine *hedgehog* gene. *Development* **120**, 3339-3353.

Cohn, M. J., Izpisua-Belmonte, J. C., Abud, H., Heath, J. K. and Tickle, C. (1995). Fibroblast growth factors induce additional limb development from the flank of chick embryos. *Cell* **80**, 739-746.

Crossley, P. H. and Martin, G. R. (1995). The mouse *Fgf8* gene encodes a family of polypeptides and is expressed in regions that direct outgrowth and patterning in the developing embryo. *Development* **121**, 439-451.

Echelard, Y., Epstein, D. J., St-Jacques, B., Shen, L., Mohler, J., McMahon, J. A. and McMahon, A. P. (1993). *Sonic hedgehog*, a member of a family of putative signaling molecules, is implicated in the regulation of CNS polarity. *Cell* **75**, 1417-1430.

Fallon, J. F. and Crosby, G. M. (1975). Normal development of the chick wing following removal of the polarizing zone. *J. Exp. Zool.* **193**, 449-455.

Fallon, J. F., López, A., Ros, M. A., Savage, M. P., Olwin, B. B. and Simandl, B. K. (1994). FGF-2: apical ectodermal ridge growth signal for chick limb development. *Science* **264**, 104-107.

Feldman, B., Poueymirou, W., Papaioannou, V. E., DeChiara, T. M. and Goldfarb, M. (1995). Requirement of FGF-4 for postimplantation development. *Science* **267**, 246-249.

Fields-Berry, S. C., Halliday, A. L. and Cepko, C. L. (1992). A recombinant retrovirus encoding alkaline phosphatase confirms clonal boundary assignment in lineage analysis of murine retina. *Proc. Nat. Acad. Sci. USA* **89**, 693-697.

Hébert, J. M., Basilico, C., Goldfarb, M., Haub, O. and Martin, G. (1990). Isolation of cDNAs encoding four mouse FGF family members and characterization of their expression patterns during embryogenesis. *Dev. Biol.* **138**, 454-463.

Jackson-Grusby, L., Kuo, A. and Leder, P. (1992). A variant *limb deformity*

transcript expressed in the embryonic mouse limb defines a novel formin. *Genes Dev.* **6**, 29-37.

Kaufman, M. H. (1992). *The Atlas of Mouse Development*. San Diego: Academic Press, Inc.

Kleinebrecht, J., Selow, J. and Winkler, W. (1982). The mouse mutant limb-deformity (ld). *Anatomischer Anzeiger* **152**, 313-324.

Krauss, S., Concordet, J.-P. and Ingham, P. W. (1993). A functionally conserved homolog of the Drosophila segment polarity gene *hh* is expressed in tissues with polarizing activity in zebrafish embryos. *Cell* **75**, 1431-1444.

Laufer, E., Nelson, C. E., Johnson, R. L., Morgan, B. A. and Tabin, C. (1994). *Sonic hedgehog* and *fgf-4* act through a signaling cascade and feedback loop to integrate growth and patterning of the developing limb bud. *Cell* **79**, 993-1003.

Maas, R., Elfering, S., Glaser, T. and Jepeal, L. (1994). Deficient outgrowth of the ureteric bud underlies the renal agenesis phenotype in mice manifesting the *limb deformity* (*ld*) mutation. *Dev. Dynamics* **199**, 214-228.

Maas, R. L., Zeller, R., Woychik, R. P., Vogt, T. F. and Leder, P. (1990). Disruption of formin-encoding transcripts in two *limb deformity* alleles. *Nature* **346**, 853-855.

Niswander, L., Jeffrey, S., Martin, G. R. and Tickle, C. (1994). A positive feedback loop coordinates growth and patterning in the vertebrate limb. *Nature* **371**, 609-612.

Niswander, L. and Martin, G. R. (1992). FGF-4 expression during gastrulation, myogenesis, limb, and tooth development in the mouse. *Development* **114**, 755-768.

Niswander, L. and Martin, G. R. (1993). FGF-4 regulates expression of *Evx-1* in the developing mouse limb. *Development* **119**, 287-294.

Niswander, L., Tickle, C., Vogel, A., Booth, I. and Martin, G. R. (1993). FGF-4 replaces the apical ectodermal ridge and directs limb outgrowth and patterning of the limb. *Cell* **75**, 579-587.

Parr, B. A. and McMahon, A. P. (1995). Dorsalizing signal *Wnt-7a* required for normal polarity of D-V and A-P axes of mouse limb. *Nature* **374**, 350-353.

Riddle, R. D., Johnson, R. L., Laufer, E. and Tabin, C. (1993). *Sonic hedgehog* mediates the polarizing activity of the ZPA. *Cell* **75**, 1401-1416.

Roelink, H., Augsburger, A., Heemskerk, J., Korzh, V., Norlin, S., Ruiz i Altaba, A., Tanabe, Y., Placzek, M., Edlund, T., Jessell, T. M. and Dodd, T. (1994). Floor plate and motor neuron induction by *vhh-1*, a vertebrate homolog of *hedgehog* expressed by the notochord. *Cell* **76**, 761-775.

Rosen, B. and Beddington, R. S. P. (1993). Whole-mount *in situ* hybridization in the mouse embryo: gene expression in three dimensions. *Trends in Genetics* **9**, 162-167.

Saunders, J. W. (1948). The proximo-distal sequence of origin of the parts of the chick wing and the role of the ectoderm. *J. Exp. Zool.* **108**, 363-404.

Saunders, J. W. and Gasseling, M. (1968). Ectodermal-mesenchymal interaction in the origin of limb symmetry. In *Epithelial-Mesenchymal Interaction* (eds. R. Fleischmayer and R. E. Billingham), pp. 78-97. Baltimore: Williams and Wilkins.

Savage, M. P., Hart, C. E., Riley, B. B., Sasse, J. and Olwin, B. B. (1993). Distribution of FGF-2 suggests it has a role in chick limb bud growth. *Dev. Dynamics* **198**, 159-170.

Saxen, L. (1987). *Organogenesis of the Kidney*. Cambridge: Cambridge University Press.

Sinn, E., Muller, W., Pattengale, P., Tepler, I., Wallace, R. and Leder, P. (1987). Coexpression of MMTV/v-Ha-*ras* and MMTV/c-*myc* genes in transgenic mice: synergistic action of oncogenes in vivo. *Cell* **49**, 465-475.

Summerbell, D. (1974). A quantitative analysis of the effect of excision of the AER from the chick limb-bud. *J. Embryol. Exp. Morph.* **32**, 651-660.

Summerbell, D., Lewis, J. H. and Wolpert, L. (1973). Positional information in chick limb morphogenesis. *Nature* **244**, 492-495.

Tabin, C. J. (1991). Retinoids, homeoboxes, and growth factors: toward molecular models for limb development. *Cell* **38**, 627-637.

Tickle, C. (1981). The number of polarizing region cells required to specify additional digits in the developing chick wing. *Nature* **289**, 295-298.

Tickle, C. and Eichele, G. (1994). Vertebrate limb development. *Ann. Review Cell Biol.* **10**, 121-152.

Tickle, C., Summerbell, D. and Wolpert, L. (1975). Positional signalling and specification of digits in chick limb morphogenesis. *Nature* **254**, 199-202.

Trumpp, A., Blundell, P. A., Pompa, J. L. d. l. and Zeller, R. (1992). The chicken *limb deformity (ld)* gene encodes nuclear proteins expressed in specific cell types during morphogenesis. *Genes Dev.* **6**, 14-28.

Vogel, A. and Tickle, C. (1993). FGF-4 maintains polarizing activity of posterior limb bud cells *in vivo* and *in vitro*. *Development* **119**, 199-206.

Vogt, T. F., Jackson-Grusby, L., Wynshaw-Boris, A. J., Chan, D. C. and Leder, P. (1992). The same genomic region is disrupted in two transgene-induced *limb deformity* alleles. *Mammalian Genome* **3**, 431-437.

Wilkinson, D. G. (1992). Whole mount *in situ* hybridization of vertebrate embryos. In *In Situ Hybridization: A Practical Approach* (eds. D. G. Wilkinson), pp. 75-83. Oxford.

Woychik, R. P., Generoso, W. M., Russell, L. B., Cain, K. T., Cacheiro, N. L. A., Bultman, S. J., Selby, P. B., Selby, M. E., Dickinson, M. E., Hogan, B. L. M. and Rutledge, J. C. (1990a). Molecular and genetic charaterization of a radiation-induced structural rearrangement in mouse chromosome 2 causing mutations at the *limb deformity* and *agouti* loci. *Proc. Nat. Acad. Sci. USA* **87**, 2588-2592.

Woychik, R. P., Maas, R. L., Zeller, R., Vogt, T. F. and Leder, P. (1990b). 'Formins': proteins deduced from the alternative transcripts of the *limb deformity* gene. *Nature* **346**, 850-853.

Woychik, R. P., Stewart, T. A., Davis, L. G., D'Eustachio, P. and Leder, P. (1985). An inherited limb deformity created by insertional mutagenesis in a transgenic mouse. *Nature* **318**, 36-40.

Yang, Y. and Niswander, L. (1995). Interaction between the signaling molecule WNT7a and SHH during vertebrate limb development: dorsal signals regulate anteroposterior patterning. *Cell* **80**, 939-947.

Zeller, R., Jackson-Grusby, L. and Leder, P. (1989). The *limb deformity* gene is required for apical ectodermal ridge differentiation and anteroposterior limb pattern formation. *Genes Dev.* **3**, 1481-1492.

(Accepted 20 June 1995)